The Journal of Physical Chemistry B

 VOLUME 103, NUMBER 27, JULY 8, 1999

ARTICLES

Directing Silver Nanoparticles into Colloid−Surfactant Lyotropic Lamellar Systems

Wei Wang,[†] Shlomo Efrima,*[,†] and Oren Regev[‡]

Departments of Chemistry and Chemical Engineering, Ben-Gurion University of the Negev, Beer-Sheva 84105, Israel

Received: July 22, 1998; In Final Form: April 12, 1999

We introduce hybrid systems composed of silver nanoparticles and ordered lamellar phases of the water/SDS/hexanol/dodecane system. Silver colloids are selectively directed either to the aqueous layer or to the organic layer for the same basic system and are confined within the lamellae. In the case of hydrophobic particles, some penetration into the hydrophobic region of the surfactant layer is noted. The composites are investigated by SAXS and UV−visible absorption spectroscopy. The evolution of the periodicity was studied in detail, varying the different parameters of the phase diagram. It was found that the incorporation of silver colloids does not noticeably disturb the basic smectic structure, except that the interlamellar spacing changes. With the colloid in the aqueous region or in the organic region, the stability region of the L_α phase is modified only slightly compared to that when the colloids are absent. The formation and the stability of the hybrid systems are explained by a delicate balance of electrostatic repulsive, VDW attractive, and Helfrich long-range repulsive forces.

Introduction

The assembly of ordered systems of inorganic matter in organic matrixes is of recent practical and fundamental interest.[1−4] Lyotropic lamellar phases, in which amphiphilic molecules self-assemble to form layers that stack with a long-range periodicity, are a promising system to achieve that goal and are of current concern, particularly due to the ability of some systems to be stable up to large solvent-to-surfactant ratios.[5,6] Very recently, single-phase systems combining a lyotropic lamellar phase and oil- or water-stabilized magnetic particles have been described by Fabre et al.[7−11] and Menager et al.,[12] respectively. In the present report, we extend this pioneering work to silver colloids with varying and controllable surface properties. In particular, we demonstrate the existence of stable lyotropic lamellar systems doped either by aqueous colloidal silver particles (hydrophilic hydrosol), or by organic colloidal silver particles (hydrophobic organosol), or, in less stable systems, with both aqueous and organic colloidal silver particles present simultaneously. We are able to direct the nanoparticles selectively to the water or the oil layer of a lamellar phase. The nanoscale solid particles are confined in the thin nanoscale space in or between the lyotropic membranes. We use the sodium dodecyl sulfate (SDS/water)/hexanol/dodecane pseudoternary system as the undoped lamellar phase. The basic idea of this study is to understand how a metal colloidal dispersion can incorporate into a liquid structured phase and in what ways does it affect the stability and the order of this complex system. The longer range goal is to develop methodologies for directing solid nanoparticles into predetermined specific physicochemical environments. In addition, one might make use of the optical properties (linear and nonlinear) of the metal particles, much as one might utilize the magnetic properties of the iron oxide−SDS systems. In fact, it would be interesting to combine the magnetic particles and the metal particles together in one lamellar system.

* To whom correspondence should be addressed.
[†] Department of Chemistry.
[‡] Department of Chemical Engineering.

10.1021/jp983125n CCC: $18.00
Published on Web 06/19/1999

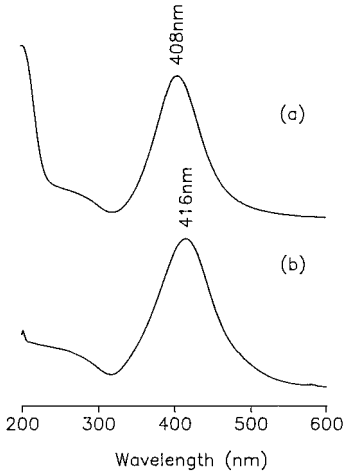

Figure 1. UV−visible spectra of colloidal silver particles dispersed in (a) water and (b) dodecane.

Experimental Materials and Methods

$AgNO_3$ (99+%), $NaBH_4$ (99%), dodecane (99+%), and oleic acid (>99%) were purchased from Aldrich. H_3PO_4 (85%) was obtained from Merck. NaOH (analytical grade) was provided by Frutarom, and 1-hexanol (>99%, GC) was from Fluka. All reagents were used without further purification (unless stated otherwise). Water was of ~18 MΩ cm resistivity, obtained from a Barnsted E-pure water purifier.

UV−visible spectra were taken with a 8452A HP diode array spectrophotometer in the range 190−820 nm, with a resolution of 2 nm. A variable-path cuvette with lithium fluoride windows was used.

Small-angle X-ray scattering (SAXS) experiments were performed using Ni-filtered Cu Kα radiation (0.154 nm) from a Seifert ID 3000 sealed tube X-ray generator operating at 40 kV and 40 mA. The sample was inserted into 1.5 mm glass capillaries which are then sealed with an epoxy glue. The scattering vector, q, is defined as $q = 4\pi \sin(2\theta/\lambda)$, where 2θ is the scattering angle and λ is the wavelength.

Results and Discussion

1. Silver Sols. The silver colloidal sols are prepared according to methods described elsewhere.[13]

Typically, a reddish-brown hydrophilic silver colloidal dispersion in water, with a volume fraction of 0.005% Ag, is obtained by mixing with vigorous stirring at ice cold temperature 1 part of 1×10^{-2} M silver nitrate and another equivolume part of 4×10^{-2} M sodium borohydride containing 2.5×10^{-3} M sodium oleate. This procedure gives negatively charged (surface charge density ~0.02 C/m^2 [13]) hydrophilic particles, capped by a shell of adsorbed sodium oleate.

Organosols are prepared from the hydrosol by adding dropwise with vigorous stirring 0.2 M H_3PO_4 (reaching pH values of 3−5 in the aqueous phase) to a mixture of the silver hydrosol and an equivolume immiscible organic solvent, such as dodecane or cyclohexane.[13] An immediate phase transfer of the silver particles from water to the organic phase is induced.

UV−visible spectra of the sols are given in Figure 1. The silver particles dispersed in water and dodecane exhibit characteristic extinction maxima at 408 ± 2 and 416 ± 4 nm, respectively. The extinction is due to a localized plasmon resonance of the silver particles. The symmetric and narrow spectra in Figure 1 are characteristic of nonaggregated spherical silver particles with a narrow size distribution.[14−17] The shift of the maximum of the absorption band for the hydrosol compared to the organosol is due to the different interactions with the ambient solvent.[18,19]

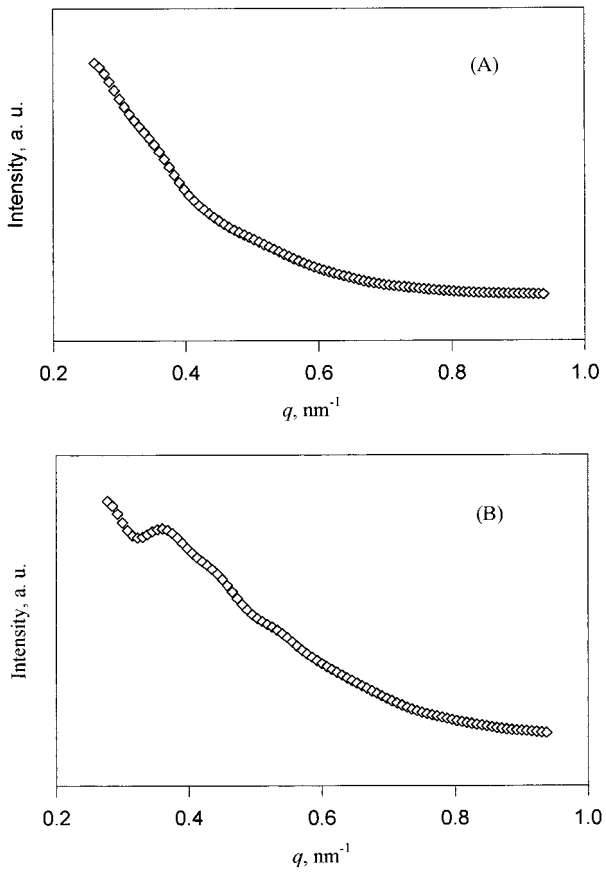

Figure 2. Scattering curves (SAXS) of (A) hydrophilic silver colloid in water, $\langle d \rangle = 5.0$ nm, and (B) hydrophobic silver colloid in cyclohexane, $\langle d \rangle = 4.4$ nm.

Figure 2 shows the SAXS spectra of the sols. We do not know the origin of the reproducible hump in Figure 2B. It might be related to a form factor, though we could not fit that of a solid sphere. A hollow particle might give such a signature, but our particles are full, not hollow.

Assuming dilute, noninteracting, and globular monodisperse particles, the size of the particles may be calculated based on the Guinier approximation.[20] The above-mentioned hump does not affect the analysis of the Guinier plot, as the calculation uses only very low q values. We find that the average diameters of silver particles, $\langle d \rangle$, are 4.4 and 5.0 nm in the hydrophobic and hydrophilic sols. The sizes are in good agreement with the TEM results, which give narrow size distributions, with average diameters of 4.4 and 5.0 nm and standard deviations of 1.2 and 1.9 nm, respectively.[13] These silver colloidal dispersions are stable at room temperature over periods longer than 3 months. Electrophoresis measurements show that the hydrophilic Ag particles are negatively charged.[13]

2. Lyotropic Lamellar Phase. 2.1. Construction of Doped Lamellar Phases. A lamellar phase is a periodic packing of alternating water layers separated by a membrane consisting of both surfactant and cosurfactant molecules. In oil-swollen lamellar systems, the two leafs of the bilayer are separated by the oil. In this report, the undoped lamellar phases are a quaternary system composed of water, SDS as the surfactant, hexanol as a cosurfactant, and dodecane as the oil component when it is present. In practice, we fix the weight ratio of water/surfactant (W/S) so that the quaternary system may be regarded as a pseudoternary system. This pseudoternary system exhibits

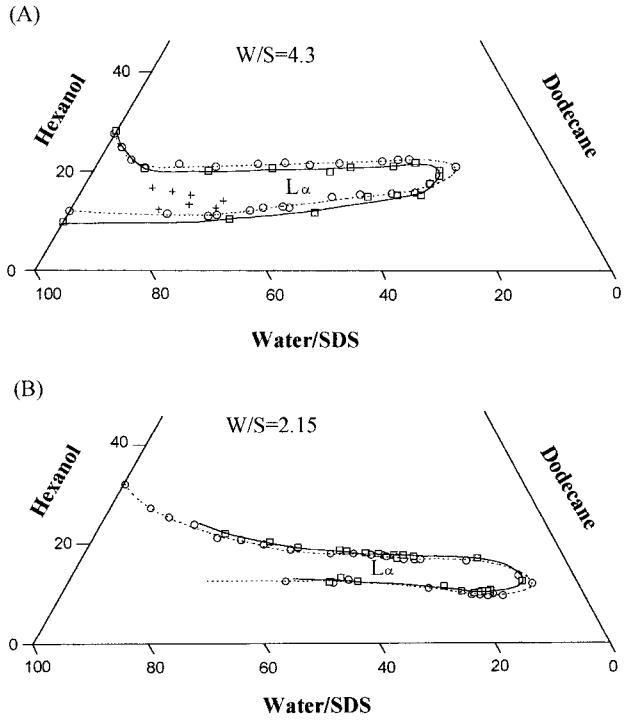

Figure 3. Phase diagrams (volume fraction) of the pseudoternary system (water + SDS)/hexanol/dodecane (A) at a weight ratio W/S = 4.3, doped by hydrophilic silver sol, and (b) at a weight ratio W/S = 2.15, doped by hydrophobic silver sol. [Ag] = 5×10^{-3} M. The points denoted by circles and squares represent the boundary of the undoped and doped systems, respectively. The crosses denote points of a biphasic region with two intermixed birefringent phases. The lines are drawn freehand as a guide to the eye: undoped pure lamella, dashed line; doped lamella, full line.

a lamellar structure over a large domain of water and surfactant concentrations at room temperature.[21−26] Within the monophasic domain, the lamellar periodicity (d_l) may vary from several nanometers to several tens of nanometers, by changing the organic layer thickness, d_o, while keeping constant the thickness of the water layer, d_w, and that of the surfactant layer, d_s. This is easily carried out by controlling the relative volume of the organic liquid.

In Figure 3 we show the lamellar region of the pseudoternary phase diagram as determined by birefringence and SAXS measurements. The general location of the L_α region and its shape are roughly similar to those reported by Bellocq et al.[6] though there are differences in the details. In addition, we find that a zone inside the L_α region (Figure 3) is biphasic, with two coexisting birefringent liquid crystals. A detailed study of this is forthcoming. In the present report, we restrict ourselves to regions that are strictly monophasic lamellar, unless noted otherwise.

We construct the various silver-doped systems in the following ways: The first is by using a silver hydrosol instead of pure water, forming a hydrophilic silver-particle-doped lamellar phase. A second approach is to swell a preassembled lamellar phase with a silver organosol, instead of the pure organic solvent. This yields a hydrophobic silver-particle-doped lamellar phase. A combination of the above two procedures is used to produce a lamellar phase that is doped by both hydrophilic and hydrophobic silver particles simultaneously. Generally, we use a silver ion concentration of [Ag] = 5×10^{-3} M (in terms of silver atoms), as this is a typical concentration for stable metallic colloids. We are able to prepare and work at a 100-fold higher concentration, i.e., volume fractions of 0.5%. However, using the lower concentration avoids perturbation of the lamellae by competition over the surfactant molecules by the membranes and the coating needed to stabilize the particles.

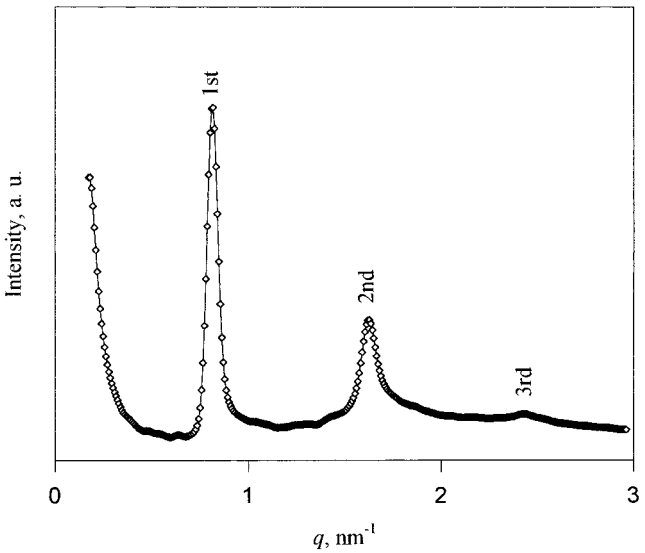

Figure 4. Scattering curve (SAXS) of a hydrosol/SDS/hexanol system (W/S = 4.3). [Ag] = 5×10^{-3} M.

The lamellar phase boundaries of the silver-nanoparticle-doped (water + SDS)/hexanol/dodecane system at fixed W/S weight ratios are determined by the following procedure: The mixture of any designated composition in a sealed tube is carefully mixed by a vortex mixer for about a minute, air bubbles are removed by centrifugation, and it is allowed to equilibrate at a constant temperature. After 12 h at room temperature (25 ± 1 °C), the number of phases and their characteristics are checked by observation of the birefringence between crossed polarizers and then by SAXS measurements. We studied the effect on the phase diagram of two Ag concentrations of sols (5×10^{-3} and 1×10^{-4} M, *i.e.*, volume fractions in the aqueous region of 0.005% and 0.001%, respectively). At W/S = 4.3 and [Ag] = 5×10^{-3} M, the incorporation of hydrophilic silver particles shifts the whole diagram very slightly but consistently toward a water and surfactant richer and cosurfactant leaner area (Figure 3A). At this composition, the colloid−lamellar hybrid is stable for at least a month. At W/S = 2.15 and [Ag] = 5×10^{-3} M, the incorporation of hydrophobic silver particles also yields a highly stable hybrid system. The colloid slightly modifies the boundaries of the phase diagram (Figure 3B), shifting the lamellar region to the hexanol-rich corner.

At [Ag] = 1×10^{-4} M (0.001% silver volume fraction), there is hardly any effect for both W/S ratios, and the diagrams are practically the same as that of the initial undoped phase in both cases (not shown). Preliminary results show that the hitherto unknown biphasic region which we found (Figure 3A) (usually considered to be a pure lamellar region[27]) is composed of a mixture of lamellar and hexagonal phases. The silver concentrates preferentially only in the hexagonal component, avoiding the lamellar regions altogether.

2.2. Effect of the Water Layer Thickness on Systems Doped with Hydrophilic Particles. A typical SAXS pattern of a colloid-doped lamellar system is given in Figure 4. The three reflections observed agree with a lamellar symmetry.

A lamellar phase is characterized by its repetition distance, d_l. Assuming no interpenetration, it is given by $d_l = d_w + d_o + d_s$, where the subscripts w, o, and s refer to the water layer, the organic phase, and the surfactant membrane, respectively. The

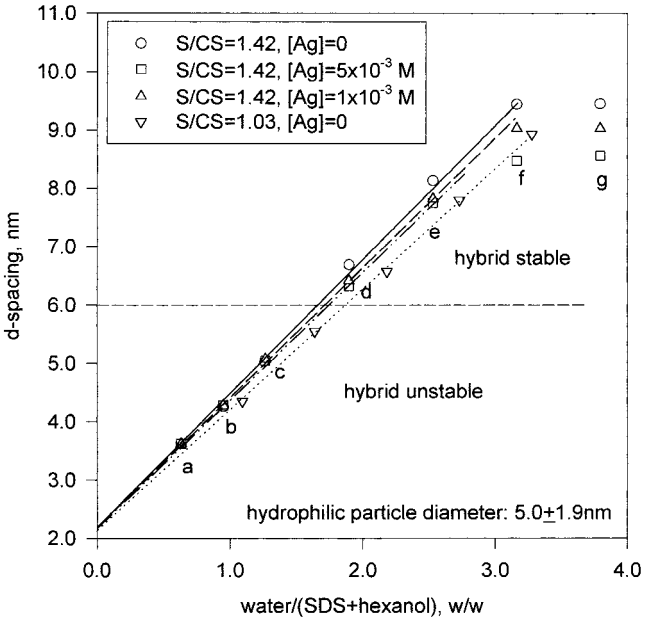

Figure 5. Lamellar periodicity of water (or Ag colloid)/SDS/hexanol systems determined using SAXS at different water content fractions and fixed weight ratio S/CS. S/CS = 1.42. Pure lamellar phase, circles; with a hydrosol ([Ag] = 1×10^{-3} M), triangles; with a hydrosol ([Ag] = 5×10^{-3} M), squares; S/CS =1.03, pure lamellar phase, inverted triangles. The points a−g refer to Figure 6. The experimental uncertainty is about one-third the size of the symbols.

structural characteristics of the phase can be derived from SAXS, as the position (q_{max}) of the first Bragg peak is related to the lamellar spacing, $d_l = 2\pi/q_{max}$.[27] In the following, we discuss the behavior of the colloid−surfactant hybrid system when the thickness of the various layers is changed by several different means. Note that not all the compositions utilized are represented in the phase diagrams of Figure 3.

2.2.1. Water Swelling at Different Surfactant-to-Cosurfactant Weight Ratios (S/CS). Interlamellar Distances. In Figure 5 the calculated interlayer spacings are plotted against the weight ratio of water (or hydrosol) at fixed S/CS (SDS/hexanol) weight ratios of 1.42, and 1.03, without any additional organic solvent. The SAXS measurements were taken 1−3 days after preparing the samples (and before phase separation sets in; see below). The resulting straight line at lower water content represents one-dimensional water swelling of a lamellar liquid-crystalline phase. By extrapolating to zero water concentration, the average surfactant membrane thickness is determined to be 2.2 nm, regardless of the surfactant/cosurfactant weight ratios. Alternatively, the slope of the lamellar repeating distance versus the reciprocal of the total hydrophobic volume (including the cosurfactant and the hydrophobic tails of the SDS − there is no oil in this set of experiments) yields a bilayer thickness of 2.11 ± 0.03 nm. This value is low compared to a theoretically derived value of 3.3 nm of an hydrocarbon chain bilayer composed of *all-trans*-SDS aligned normal to the layer. This difference might be understood in terms of interdigitation of the hydrocarbon chains and their liquid nature. In Figure 5 we notice a departure from the linear relation at high water content, accompanied by the appearance of another nonbirefringent isotropic phase. The lamellar phase persists with a constant spacing, indicating a crossing of the boundary of the lamellar phase.

Comparing a pure lamellar phase with those doped with Ag (Figure 5), we find that at lower water content, the incorporation of Ag particles almost does not disturb the lamellar periodicity, while at higher water content it decreases the lamellar spacing. The higher the concentration of the Ag colloids, the larger is the effect.

We would like to discuss now a model that assumes that the changes in the spacing are predominantly determined by particle−membrane or particle−particle interactions across the membrane, which bring about a penetration of the surfactant adsorbed on the particles into membrane, disturbing its structure. Indeed particles with the adsorbed surfactant are larger than the ∼6 nm water spacing at the onset of stability (see below). We mention specifically the particle−particle and particle−membrane VDW attractions and the longer range interparticle and particle−headgroup electrostatic repulsions. It seems that at the small membrane thickness (without oil), the former overbalances the latter. The ensuing contractile pressure on the membrane results in its compression and shrinkage, as seen in Figure 5. This compression results in a larger area of the membrane (i.e., larger headgroup area), accommodating thinner water layers. Thus, the decrease in the lamellar spacing (by about 1 nm) could be due to two contributions: the direct shrinkage of the bilayer and the indirect thinning of the water layers. One can quantify these effects using a simple model assuming that the density of the membrane is constant and that it is close-packed. The total volume of the bilayer, V_s, is given by

$$V_s = Ad_s \tag{1}$$

where A is the area of the membrane. Similarly, the total volume of the water layer, V_w, is given by

$$V_w = Ad_w \tag{2}$$

with the same area as that of the membrane.

The change in the spacing is given by

$$\delta d_l = \delta d_s + \delta d_w \tag{3}$$

By using eqs 1 and 2 in eq 3, we get

$$\delta d_l = \left(\frac{V_w}{V_s} + 1\right)\delta d_s = \left(\frac{W}{S}\frac{\rho_s}{\rho_w} + 1\right)\delta d_s \tag{4}$$

with ρ being the corresponding density of water, w, and the surfactant, s, and W/S is their weight ratio. In the samples of Figure 5, W/S varies between ∼1.2 and 5.4 (it is proportional to the water/(SDS + hexanol) ratio) so that any small change in the width of the surfactant layer, d_s, is amplified by these ratios (the density ratio is close to unity but would tend to increase the amplification factor even further). Thus, it is expected that the effect on d_l will increase as W/S increases, as is indeed seen in Figure 5. Furthermore, the largest spacing change is of ∼1 nm, at water/(SDS + hexanol) = 3.2 (W/S = 5.4). Using eq 4 shows that this rather large decrease requires only a small compression of the surfactant bilayers, by ∼0.16 nm. The slightly larger headgroup area is consistent with repulsive interactions between the similarly charged particles and headgroups.

What is perhaps surprising about the changes in the spacing is not their magnitude, as they reflect quite minor changes in the surfactant layer itself, but the fact that a very small concentration of silver particles brings about such changes. At a concentration of 5×10^{-3} M silver, we have $\sim 0.9 \times 10^5$ particles of 5 nm diameter per cm^3, giving an average interparticle distance of ∼100 nm (and volume fractions of 10^{-5} silver). At these distances, the VDW energies of interaction between two spheres with the Hamaker constant for silver (*A*

$= (30-40) \times 10^{-20}$ J)[28] are typically 6×10^{-15} erg, much smaller than thermal energies at room temperature. However, one cannot rule out VDW interactions only on the basis of the average interparticle distance, as clustering might be present. The interaction energy of two particles directly across a surfactant bilayer, at a distance of 3 nm, is $\sim 2 \times 10^{-13}$ erg, exerting strong forces perpendicular to the membrane. These relatively strong interparticle attraction forces might be manifested in the clustering of the silver particles in the lamellar phase we observe for higher silver concentrations (∼0.1 M). Thus, in principle, the interparticle VDW interactions *across the membrane* seem to be sufficiently strong, and a small restructuring of the bilayer can be manifested in much larger changes in the overall lamellar spacing. The low silver concentration in the system might attenuate these effects to some (unknown) degree.

The VDW interaction between the silver particles and the membrane itself can also be significant, and its effect should be considered. It is true that the pertinent Hamaker constant between a metal particle and a membrane is up to ∼10−50-fold weaker than for the metal−metal interaction.[28] However, the particle−membrane distance is at most a few nanometers, about 200-fold smaller than for the particle−particle average distance at the low silver concentrations, as discussed above. Thus, we would expect the particle−membrane VDW attraction energy to be larger than $\sim 4 \times 10^{-14}$ erg, i.e., of the order of kT or larger. This is sufficient to have a significant effect on the lamellae. This rough estimate neglects the screened electrostatic repulsion between the negatively charged sliver particles and the anionic headgroups of the surfactants in the membrane.

In principle, competition over the surfactant molecules between the silver particles and the bilayers could also affect the bilayer structure and thickness. However, considering the chemistry of the colloids and the low volume fraction we use, such effects are expected to be small. First, the colloids are prepared with a coating of oleate surfactant molecules. There is not much free space on the particle surfaces to accommodate additional anionic SDS.[13] Thus, the particles are not expected to pull SDS out of the membranes. Furthermore, the amount of oleate (1.25×10^{-3} to 0.25×10^{-3} M in the aqueous region) compared to that of SDS (∼1−2 M, with W/S = 4−2) is so low that even if there is some SDS/oleate exchange, its effect on the lamellae is expected to be negligible.

Stability. By using hydrophilic Ag particles to dope the system, we find that the stability of the particles in the doped phase depends on the W/S ratio, reflecting, perhaps, the water layer thickness and its additional ability to accommodate the 4−5 nm silver particles. This conjecture is supported by experimental findings as follows:

Figure 6 shows the UV−visible spectra of samples with [Ag] $= 5 \times 10^{-3}$ M corresponding to the a−g points in Figure 5. At *d* spacing below 6 nm, i.e., water layer thickness < ∼3.8 nm, the spectra in Figure 6a−c exhibit a broad and flat feature extending well into the red. This behavior is characteristic of strongly interacting silver particles or conglomerates.[29] Fresh samples appear homogeneously gray, and only after several days is a complete phase separation between an undoped phase and black aggregates of particles observed. The SAXS spectra show that the periodic structure of the separated lamellar phase has practically the same spacing as in the pure surfactant lamellar phase. This suggests that the silver particles are squeezed out of the lamellar layers when the thickness of the water layer (∼3.8 nm) is simply too narrow for the ∼4−5 nm Ag colloidal particles. At a *d* spacing of ∼6.3 nm, i.e., water layer thickness

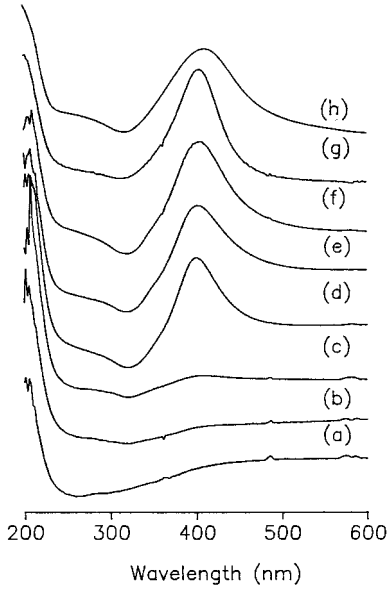

Figure 6. UV−visible spectra of the water/SDS/hexanol system doped with hydrosol containing [Ag] $= 5 \times 10^{-3}$ M at different water contents and a fixed molar ratio SDS/hexanol = 1:2. The phase composition in spectra a−g correspond to the a−g points in Figure 5, and spectrum h is the absorption of an Ag colloid in pure SDS micelles (W/S = 4.3).

of ∼4 nm, the sample is yellowish gray and its absorption spectrum (Figure 6d) exhibits an absorption maximum at 400 nm with a pronounced absorption wing toward long wavelengths, demonstrating the mixed characteristics of individual separated silver particles as well as aggregated colloids. After aging for a few days, cloudy black aggregates are found dispersed in the clearly yellowish sample, indicating some exclusion of aggregated silver, in parallel with a colloid (probably the smaller particles) retained in the lamellae. However, at *d* spacings above ∼7 nm, the absorption wings at long wavelengths become weak (Figure 6e and f) and eventually disappear (Figure 6g). At the high water content, the spectrum exhibits a well-defined absorption band at 406 nm, characteristic of individual silver colloidal particles. The absorption peak is blue-shifted by 6 nm from the position for particles in pure SDS micelles, is narrower, and is more symmetric, implying a smaller degree of aggregation within the lamellar phase.

All the spectra of the samples corresponding to Figures 5 and 6 display two Bragg peaks for the pure lamellar phase, indicating a well-defined, long-range order. The first-order peaks are very sharp at low water content, exhibiting the behavior of an electrostatically controlled lamellar phase.[30,22] With increasing water content, the Bragg peaks broaden and exhibit increasing scattering intensity when *q* approaches zero, indicative of a weakening of the electrostatic interactions between membranes. When hydrophilic particles dope the lamellar phase, at high water content, the Bragg peaks are narrower than those of the corresponding pure lamellar phase. Even the third Bragg peak can be observed (Figure 4). This once again indicates a stronger electrostatic interaction, in agreement with a repulsive electrostatic interaction between the silver particles and the surfactant headgroups.

UV−visible spectra show that the state of dispersion of the silver particles in samples d−g is still maintained in the lamellar phase for at least a month at room temperature. This stability is still apparent to the eye after 3 months. It is clear that a stable doped phase requires sufficient space between the layers (large W/S ratio); otherwise, the particles are expelled from the lamellae.

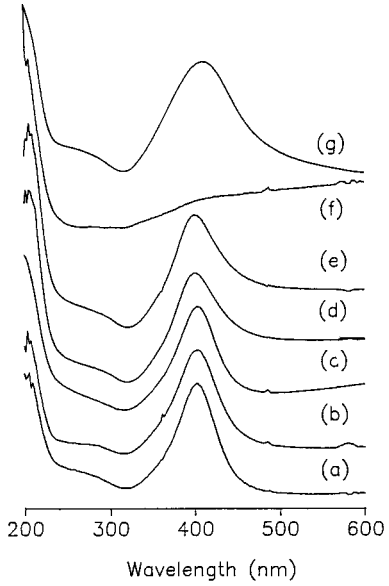

Figure 7. UV−visible spectra of the water/SDS/hexanol system doped with hydrosol containing [Ag] = 5×10^{-5} M at different hexanol contents and fixed weight ratio W/S = 4.3. The phase composition in spectra a−f is relative to the a−f points in Figure 8. Spectrum g is the absorption of Ag colloid in pure SDS micelles.

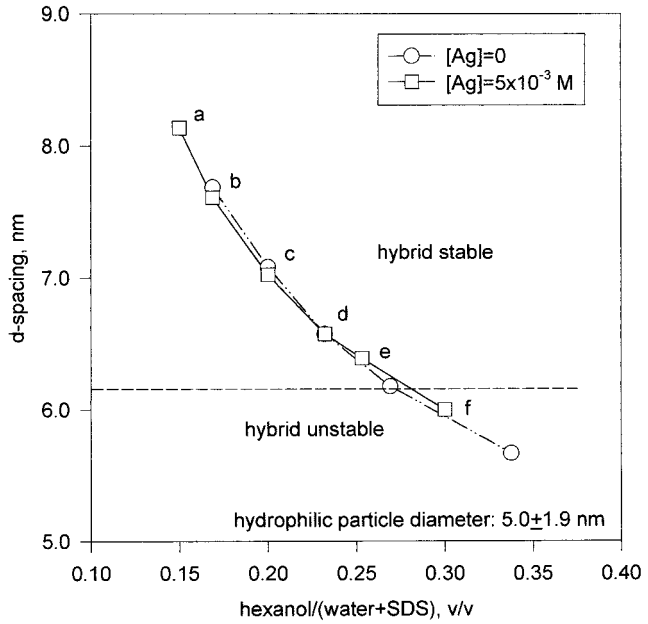

Figure 8. Lamellar periodicity of water (or Ag colloid)/SDS/hexanol systems determined using SAXS at different hexanol contents and fixed weight ratio. W/S = 4.3, pure lamellar phase, circles; with [Ag] = 5×10^{-3} M, triangles. The points a−f refer to Figure 7. The experimental uncertainty is about one-half the size of the symbols.

By using crossed-polarized optical microscopy, we find that the texture of the stable lamellar phases, both undoped and silver-doped, is very similar. They exhibit the characteristic oily streaks and plates of lamellar phases. We did not observe any conical defects in either of the samples, indicating that defects in the lamellar phases are scarce and that the incorporation of the silver particles does not change this situation significantly.

2.2.2. CS Effects. The same conclusion is arrived at when we fix the W/S weight ratio at a high value of 4.3 and change the lamellar *d* spacing by changing the cosurfactant (hexanol) content. The UV−visible absorption spectra (Figure 7) exhibit essentially the characteristic maximum of isolated particles throughout most of the range we investigated. However, it is evident that at interlayer spacings below ~7 nm (points d and e in Figure 8), some aggregation sets in as evidenced in the asymmetry of the band. Below 6 nm (Figure 8f), strong interparticle interactions are observed, totally obliterating the sharp spectrum and heralding the onset of aggregation. Note that there is no difference between the behavior of the pure and the doped systems in terms of the spacing (Figure 8).

Of course, the requirement of a ratio larger than about 1 between the interlayer spacing in the lamellar phase and the size of the doping particles is necessary but may not be sufficient for stabilizing hybrid systems in general and the one we consider here, in particular. In the next section we demonstrate this point.

2.3. Effect of the Organic Layer Thickness. *2.3.1. Water/SDS Ratio of 4.3: Hydrophilic and Hydrophobic Particles.* The lamellar phase can also be swollen by increasing its oil layer thickness at constant water layer thickness. At high organic content, in Figure 9 we find, by SAXS, a biphasic region (intermixed lamellar and hexagonal phases as revealed by SAXS and optical microscopy).

Hydrophilic Particles. In a hydrophilic Ag-doped lamellar phase, the Ag colloid initially maintains its well-dispersed state even after it is swollen by the pure organic component. Nevertheless, its stability deteriorates with increasing the relative amount of the organic component, as observed by UV−visible spectra (not shown). Perhaps the oil-swollen phase is less rigid than that formed in the absence of the organic liquid, and the kinetic (particle motion) contribution to the stabilization of the colloid is reduced (see below). This might plausibly suggest that the bending constants of single layers are smaller than that of the bilayer, leading to more significant membrane fluctuations.

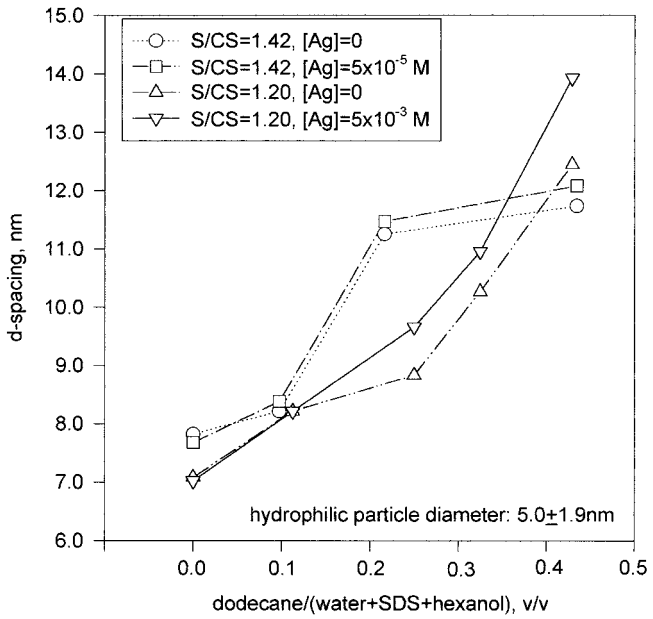

Figure 9. Lamellar *d* spacing determined using SAXS at different oil fractions for a pure (water + SDS)/hexanol/dodecane system (W/S = 4.3), circles, and a doped phase with [Ag] = 5×10^{-3} M hydrophilic colloid, squares. The experimental uncertainty is about one-half the size of the symbols.

The conclusions we described above are supported by the results we describe now. The smectic *d* spacings for the main lamellar phases present, deduced from the position of the Bragg peaks, are plotted as a function of the oil volume fraction in Figure 9. Compared to that of the pure lamellar phase, the presence of hydrophilic Ag particles ([Ag] = 5×10^{-3} M), at both S/SC ratios shown, increases the lamellar *d* spacing when

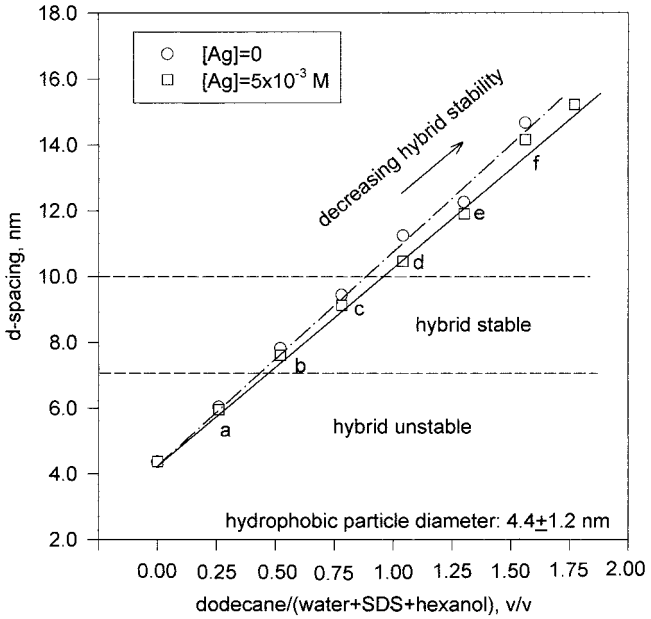

Figure 10. Lamellar periodicity determined using SAXS at different oil fractions for a pure (water + SDS)/hexanol/dodecane system (W/S = 2.15, SDS/hexanol = 1.03), circles, and a doped phase with a [Ag] = 5×10^{-3} M hydrophobic colloid, squares. The points a−f refer to Figure 11. The experimental uncertainty is about one-sixth the size of the symbols.

oil is present. Recall that in the absence of the organic solvent, the lamellar spacing is slightly smaller in the presence of the hydrosol. When the organic liquid is added, it increases the interparticle distance across the membranes in adjacent layers as well as the effective particle−membrane distance. Thus, the attractive VDW interactions (particle−membrane and particle−particle) are attenuated, compared to the repulsive long-range electrostatic interactions, leading to an expansive pressure on the membrane. This is a tentative interpretation subject to a better understanding of the biphasic behavior we observe, as mentioned above.

Hydrophobic Particles. By simply using Ag organosols instead of the pure organic component, a swollen lamellar phase doped by hydrophobic particles can be obtained. At a W/S weight ratio of 4.3 and using a Ag-dodecane sol, the maximum of the oil layer thickness (not including the surfactant bilayer) is still smaller than 3 nm, as measured by SAXS (not shown). Such a small space is not enough to contain a silver particle (4−5 nm). Therefore, we only observed an unstable hybrid lamellar phase, in which the Ag particles aggregate within a few hours or, at most, in a couple of days. This aggregation of the hydrophobic particles, however, is much slower than that of the hydrophilic particles when the space within the water layer is insufficient.

2.3.2. Water/SDS Ratio of 2.15: Hydrophobic Particles. At a water/SDS ratio of 4.3, we cannot increase the oil content sufficiently and still remain in the lamellar domain. To obtain a sufficiently large oil layer spacing compared to the size of the silver particles, we use a lower S/W weight ratio, 2.15, instead of 4.3. Figure 10 shows the oil fraction dependence of the *d* spacing for a pure lamellar system and one doped by hydrophobic Ag particles at a W/S weight ratio 2.15 and a S/CS weight ratio of 1.03. In contrast to the case of hydrophilic particles, the incorporation of hydrophobic Ag particles decreases the *d* spacing. Indeed, we do not expect any electrostatic repulsions between the hydrophobic particles and the surfactant layer. Thus, the dominant additional factor in determining the structure of the organosol-doped lamellae might be the incorporation of the particles within the surfactant layers, particle−membrane VDW attraction, and perhaps interparticle VDW attraction across the layers (which might be small considering the average distances at low silver concentrations). This would lead to smaller spacings in the system. In the case of the charged hydrophilic particles, this attraction is counterbalanced electrostatically. Note that the changes in the spacing due to the presence of the silver organosol are smaller than those we observed for a hydrosol, less than 0.5 nm compared to ∼1 nm. This is reasonable as the VDW forces with oil in the system are weaker as a result of the larger distances between the two sides of the surfactant swollen bilayers.

The UV−visible spectra of the hydrophobic Ag-doped system at various *d* spacings are shown in Figure 11. In the initial few hours, they exhibit characteristic spectra of well-dispersed Ag colloids regardless of the amount of organic solvent. It seems that for short times, the hydrophobic particles can incorporate into the lamellar phase at almost any oil content, including when oil is practically absent (e.g., at a small amount such that the thickness of the organic layer is ∼1.2 nm). At short times, the UV−visible absorption spectra closely resemble those shown in Figure 11Ab,c. But after 1 day, the hydrophobic Ag particles completely aggregate if d_o is narrower than about 3.0 nm (Figure 11Aa). This is similar to the situation we observed with the hydrophilic Ag-particle-doped system, except for the critical spacing, which was larger ($d_w \sim 5$ nm). The fact that hydrophobic particles maintain a dispersed state in the initial several hours, even for small oil spacing, instead of immediately aggregating like the hydrophilic particles indicates slow kinetics. The slowdown of the kinetics may be a result of the embedding of the hydrophobic particles in the surfactant layer itself. Evidently, the uncharged hydrophobic particles can partially penetrate into the hydrophobic region of the surfactant layers, more so than the adsorbed layers of the hydrophilic particles which are also electrostatically repelled away from the charged headgroups.

Unlike the case of hydrosols, we notice that the hydrophobic

TABLE 1: Pertinent Properties of the Colloid−Lamellar Systems

	hydrosol doping	organosol doping
W/S wt ratio	4.3	2.15
colloid particle diam, nm	5.0 ± 1.9	4.4 ± 1.2
d_w of hybrid stability, nm	<5 nm	
d_o of hybrid stability, nm		3.6−4.4 nm, gradual decline in stability up to ∼8 nm
electrostatic interactions	membrane−membrane, particle−particle, and particle−membrane	membrane−membrane
VDW interactions	membrane−membrane, particle−particle, and particle−membrane	membrane−membrane, particle−particle and particle−membrane
entropic (fluctuations) interactions	negligible compared to VDW and electrostatic without oil	considerable compared to VDW and electrostatic at larger interlayer spacings
kinetics of colloid aggregation	fast	slow, accelerating at larger interlayer spacing
penetration of particles into the membrane	none	partially into the surfactant chain domains

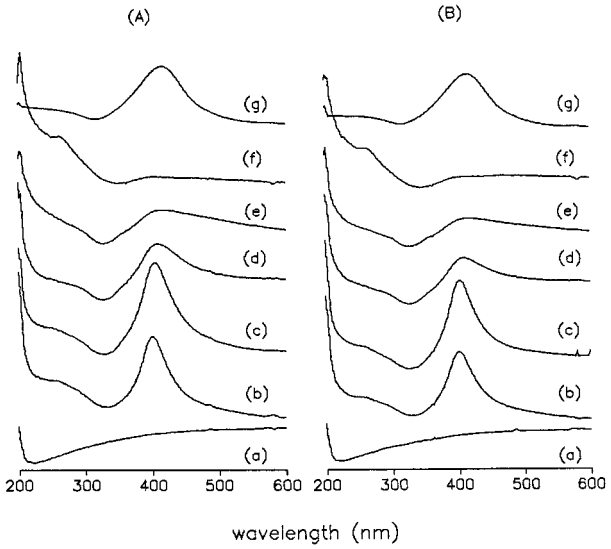

Figure 11. UV−visible spectra of the water/SDS/hexanol/dodecane system (W/S = 2.15) doped with [Ag] = 5×10^{-3} M hydrophobic colloid in (A) 1 day and (B) 1 month. The phase composition in spectra a−f corresponds to the a−f points in Figure 10, respectively. Spectrum g is the absorption of Ag colloid in dodecane at the same concentration.

silver particles tend to partly aggregate when the oil layer also becomes much wider than the particle diameter (Figure 11Ad−f, Bd−f). Hydrophobic silver particles form stable (over 3 months) lamellar-dispersed colloid systems only when the size of the silver particles is commensurate with or slightly smaller than the oil layer spacing. Similar to the hydrosol-doped lamellar phase, the incorporation of hydrophobic silver particles does not disturb the texture of the phase of the stable hybrid system as observed by crossed-polarized optical microscopy.

Helfrich[31] has proposed that thermally induced out-of-phase fluctuations of membranes in multilayer systems can lead to an effective long-range repulsive force and Israelachvili reviewed various contributions to these interactions, namely, protrusion, undulation, and peristaltic forces.[28] These interactions arise from the difference in entropy between a fluctuating "free" membrane and a restricted membrane in a multilayer system. The presence of neighboring sheets at a distance *d* restricts the thermal motion, introducing a repulsive interaction potential that balances the VDW long-range attraction between the membranes (and the particles in our case). This is usually an important consideration in discussing the stability of the lamellar phase. Solid particles in the organic phase may have a similar effect to that of closely spaced membranes. They, too, may hamper these thermal membrane fluctuations, bringing in an effective repulsion counteracting the VDW attraction. A recent study shows that an entropically stabilized phase can indeed incorporate hydrophilic particles within its lamellar matrix, whereas those particles are excluded from the electrostatically stabilized phase.[32,33] Therefore, when fluctuations become important (at high oil content), it promotes aggregation of the silver particles, leading to less hampered fluctuations of the membrane. This out-of-phase membrane motion can also affect the kinetics of particle aggregation by local convection, depletion, and enrichment (peristaltic and undulation modes). At intermediate layer spacing when the 4−5 nm particles just fit or are nearly comparable in size to it, the attractive VDW particle−membrane interactions and the interactions between the silver particles across the membrane may be the major force locally. These VDW forces, however, decrease with distance, while undulation forces change in a weaker manner.[28] Also at this composition, the particles can be kinetically protected from aggregation by their insertion

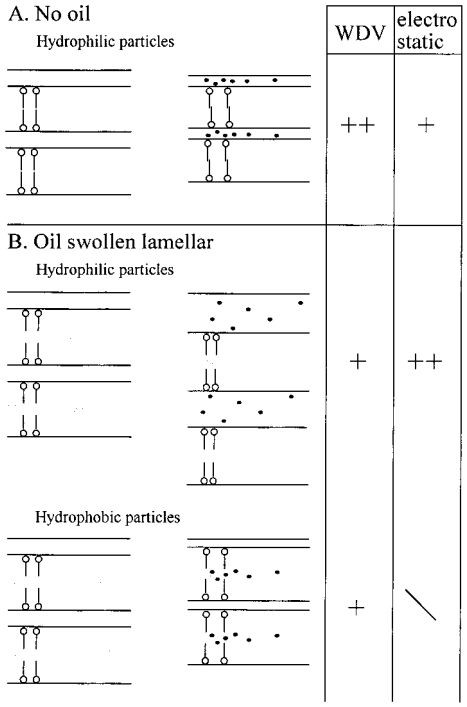

Figure 12. Interlamellar spacing and interactions—a summary cartoon. The colloid concentrations and the changes in the layer widths and headgroup areas are schematic and exaggerated. The + signs stand for (relative) importance of the VDW vs electrostatic interactions. ++ signifies a larger contribution than a single +.

into the surfactant layers or by becoming immobilized between them. Thus, there are both thermodynamic and kinetic effects working in tandem.

In the case of hydrophilic particles, these considerations do not hold, as the entropic contribution is negligible compared to the electrostatic interactions.[23]

The temperature dependence we measure supports this model. Increasing the temperature (between 5 and ∼40 °C) destabilizes the hydrophobic silver particles in the lamellar phase, in line with the growing importance of the membrane fluctuations.[28] In contrast, in this temperature range, the pure lamellar systems or the colloid alone is fully stable. Clearly the formation and the stability of these hybrid systems are determined by a delicate balance of attractive and repulsive interactions, electrostatic and VDW, as well as fluctuations (probably most importantly undulations) of the surfactant layers. These come in addition to simple considerations of water and oil layer spacing compared to the size of the particle hydrosol or organosol, respectively.

Summary

We demonstrated our ability to form combined systems of silver metal colloids and surfactant lamellar phases. We can also selectively direct the colloids to the aqueous region or to the organic region in the lamellar phase, using hydrophilic and hydrophobic particles. Hydrophilic silver particles exist only in the aqueous layers, while the hydrophobic particles also penetrate into the chain domain of the surfactant membrane. Some of the pertinent aspects of these systems are summarized in Table 1 and in Figure 12. By using UV−visible spectroscopy, we are able to check, in situ, the state of dispersion and stability of the colloids in the medium. The phase diagrams of the lamellar phase are only very weakly affected by the presence of the colloid, though there is a systematic shift of the boundary of the L_α region and the interlamellar distances are somewhat

changed. This rather small effect is expected, as the systems we study here contain a very low concentration of silver particles. Electrostatic, VDW, and membrane fluctuation forces are suggested as being important for the stabilization of these hybrid systems.

Acknowledgment. This work was supported in part by the Israel Science Foundation founded by The Israel Academy of Sciences and Humanities. We thank Svetlana Pevzner for valuable help in the SAXS measurement.

References and Notes

(1) Okada, H.; Sakata, K.; Kunitake, T. *Chem. Mater*. **1990**, *2*, 89.
(2) Murray, C. B.; Kagan, C. R.; Bawendi, M. G. *Science* **1995**, *270*, 1335.
(3) Kimizuka, N.; Kunitake, T. *Adv. Mater*. **1996**, *8*, 89.
(4) Mayya, K. S.; Patil, V.; Sastry, M. *Langmuir* **1997**, *13*, 2575.
(5) Bellocq, A. M.; Roux, D. In *Microemulsions: Structure and Dynamics*; Friberg, S. E., Bothorel, P., Eds.; CRC Press: Boca Raton, FL, 1987; p33.
(6) Bellocq, A. M. In *Physics of Complex and Supermolecular Fluids*; Safran, S. A., Clark, N. A., Eds.; John Wiley & Son: New York, 1987; p 41.
(7) Fabre, P.; Casagrande, C.; Veyssie, M.; Cabuil, V.; Massart, R. *Phys. Rev. Lett*. **1990**, *64*, 539.
(8) Fabre, P.; Ober, R.; Veyssie, M.; Cabuil, V. *J. Magn. Magn. Mater*. **1990**, *85*, 77.
(9) Quilliet, C.; Fabre, P.; Cabuil, V. *J. Phys. Chem*. **1993**, *97*, 287.
(10) Quilliet, C.; Ponsinet, V.; Cabuil, V. *J. Phys. Chem*. **1994**, *98*, 3566.
(11) Ponsinet, V.; Fabre, P.; Veyssie, M.; Cabanel, R. *J Phys. II. France* **1994**, *4*, 1785.
(12) Menager, C.; Belloni, L.; Cabuil, V.; Dubois, M.; Gulik-Krzywicki, T.; Zemb, Th. *Langmuir* **1996**, *12*, 3516.
(13) Wang, W.; Efrima, S.; Regev, O. *Langmuir* **1998**, *14*, 602.
(14) Quinten, M.; Kreibig, U. *Surf. Sci*. **1986**, *172*, 557.
(15) Creighton, J. A.; Eadon, D. G. *J. Chem. Soc., Faraday Trans.* **1991**, *87*, 3881.
(16) Petit, C.; Lixon, P.; Pileni, M. P. *J. Phys. Chem*. **1993**, *97*, 12974.
(17) Kerker, M. *J. Colloid Interface Sci*. **1985**, *105*, 297.
(18) Zeiri, L.; Efrima, S. *J. Phys. Chem*. **1992**, *96*, 5908.
(19) Kawabata, A.; Kubo, R. *J. Phys. Soc. Jpn*. **1966**, *21*, 1765.
(20) Guinier, A.; Fournet, G. *Small Angle Scattering of X-rays*; Wiley-Intersciences: New York, 1955.
(21) Roux, D.; Safinya, C. R. *J. Phys. Fr*. **1988**, *49*, 307.
(22) Safinya, C. R.; Roux, D.; Smith, G. S.; Sinha, S. K.; Dimon, P.; Clark, N. A.; Bellocq, A. M. *Phys. Rev. Lett*. **1986**, *57*, 2718.
(23) Safinya, C. R.; Sirota, E. B.; Roux, D.; Smith, G. S. *Phys. Rev. Lett*. **1989**, *62*, 1134.
(24) Roux, D.; Bellocq, A. M.; Leblanc, M. S. *Chem. Phys. Lett*. **1983**, *94*, 156.
(25) Sjoblom, J.; Blokhus, A. M.; Sun, W. M.; Friberg, S. E. *J. Colloid Interface Sci*. **1990**, *140*, 481.
(26) Di Meglio, J. M.; Dvolaitzky, M.; Taupin, C. *J Phys. Chem*. **1985**, *89*, 871.
(27) Glatter, O.; Kratky, O. *Small Angle X-ray Scattering*; Academic Press: London, 1982.
(28) Israelachvili, J. *Intermolecular & Surface Forces*, 2nd ed.; Academic Press: London, 1992.
(29) Farbman, I.; Efrima, S. *J. Phys. Chem*. **1992**, *96*, 8469.
(30) Nallet, F.; Roux, D.; Milner, S. T. *J. Phys. Fr*. **1990**, *51*, 2333.
(31) Helfrich, W. *Z. Naturforsch* **1978**, *33A*, 305.
(32) Ramos, L.; Fabre, P.; Dubois, E. *J. Phys. Chem*. **1996**, *100*, 4533.
(33) Ponsinet, V.; Fabre, P. *J Phys. Chem*. **1996**, *100*, 5035−5038.